Stress-induced birefringence in the lenses of Wide-Area Linear Optical Polarimeter-South

Ramya M Anche[a,k], Siddharth Maharana[a,b,c], A. N. Ramaprakash[a,b,e], Pravin Khodade[a], Deepa Modi[a], Chaitanya Rajarshi[a], John A. Kypriotakis[b,c], Dmitry Blinov[b,c,i], Hans Kristian Eriksen[g], Tuhin Ghosh[h], Georgia V. Panopoulou[f], Vincent Pelgrims[b,c], Raphael Skalidis[b,c], Timothy J. Pearson[e], Eirik Gjerløw[g], Nikolaos Mandarakas[b,c], Vasiliki Pavlidou[b,c], Stephen B. Potter[d,j], Anthony C. S. Readhead[e], Konstantinos Tassis[b,c], Artem Basyrov[g], Katerina Papadaki[b,c], Trygve Leithe Svalheim[g], and Ingunn K. Wehus[g]

[a]Inter-University Centre for Astronomy and Astrophysics, Post bag 4, Ganeshkhind, Pune, 411007, India
[b]Institute of Astrophysics, Foundation for Research and Technology-Hellas, Voutes, 70013 Heraklion, Greece
[c]Department of Physics, University of Crete, Voutes, 70013 Heraklion, Greece
[d]South African Astronomical Observatory, PO Box 9, Observatory, 7935, Cape Town, South Africa
[e]Cahill Center for Astronomy and Astrophysics, California Institute of Technology, Pasadena, CA, 91125, USA
[f]Hubble Fellow, California Institute of Technology, Pasadena, CA 91125, USA
[g]Institute of Theoretical Astrophysics, University of Oslo, P.O. Box 1029 Blindern, NO-0315 Oslo, Norway
[h]School of Physical Sciences, National Institute of Science Education and Research, 752050, Odisha, India
[i]Astronomical Institute, St. Petersburg State University, 198504, St. Petersburg, Russia
[j]Department of Physics, University of Johannesburg, PO Box 524, Auckland Park 2006, South Africa
[k]Steward Observatory, University of Arizona, 933N Cherry Avenue, Tucson, Arizona, 85721, USA

ABSTRACT

Two unique wide-field and high-accuracy polarimeters named WALOP (Wide-Area Linear Optical Polarimeter)-North and WALOP-South are currently under development at the Inter-University Center for Astronomy and Astrophysics (IUCAA), India, to create a large area optical polarization map of the sky for the upcoming PASIPHAE sky survey. These instruments are designed to achieve a linear polarimetric measurement accuracy of 0.1% across a field of view (FoV) of 30×30 arcminutes. The WALOP-South instrument will be installed first on a 1 m telescope at the Sutherland Observatory, where the temperatures during the night can vary between 10 to -5°C. These temperature variations and the instrument's pointing to various non-zenithal positions in the sky can introduce stress birefringence in the lenses, leading to time-varying instrumental polarization. This work estimates stress-induced birefringence due to thermal, and gravity stresses on WALOP-South lenses. Using the optomechanical model of the WALOP-South, we carried out Finite Element Analysis (FEA) simulations in *SolidWorks* software to estimate the stresses for various scenarios of temperature, telescope pointing airmass, and lens mount material (aluminum and titanium). Further, we use the stress tensor analysis to estimate the principal stresses and their directions and consequent birefringence and retardance introduced in the lenses. The stress-induced birefringence will change the optical path length for orthogonal polarization states of the beam passing through the lenses and introduce phase retardation. Overall, with the lens mount design of the instrument, we find that the retardation and consequent instrumental polarization will be within the instrumental accuracy requirements. Additionally, the stress birefringence is found to be higher for aluminum compared to titanium mounts. We further incorporated this retardance in the instrument Mueller matrix estimation to understand its effects on the polarization measurements.

Keywords: Optical polarimetry, Stress birefringence, Phase retardation, Polarimetric modelling, Polarization calibration, Muller matrix

Further author information: (Send correspondence to R.M.A)
R.M.A: E-mail: ramyaanche@arizona.edu, S.M: E-mail: sidh@iucaa.in

1. INTRODUCTION

Wide Area Linear Optical Polarimeters (WALOP-North and WALOP-South) have been designed to carry out the Polar-Areas Stellar-Imaging in Polarisation High-Accuracy Experiment (PASIPHAE) survey[1] which aims to measure the polarization of about 10^6 stars in the galactic polar regions with a polarimetric accuracy of 0.1% . WALOP-South will be mounted on a 1.0 m telescope at the South African Astronomical Observatory (SAAO) in Sutherland, and WALOP-North will be mounted on a 1.3 m telescope at the Skinakas Observatory in Greece. WALOPs are designed to achieve polarimetric sensitivity of 0.05% across a 30×30 arcminute field of view. They can measure the Stokes parameters I, q, and u in a single exposure in the $SDSS-r$ broadband and narrow band filters.

The WALOP-South instrument can be divided into three assemblies: 1. collimator, 2. polarizer, and 3. four cameras (one for each channel). The collimator assembly, beginning from the telescope focal plane, creates a pupil where the polarizer assembly is placed. The polarizer assembly splits the incoming collimated beam into four channels corresponding to 0° (O1), 45° (O2), 90° (E1), and 135° (E2) polarization angles as shown in Figure 1. Each channel has its camera, which images the entire field on a 4k×4k detector (see *Maharana et.al (2021)*[2] for more details on the optical layout)

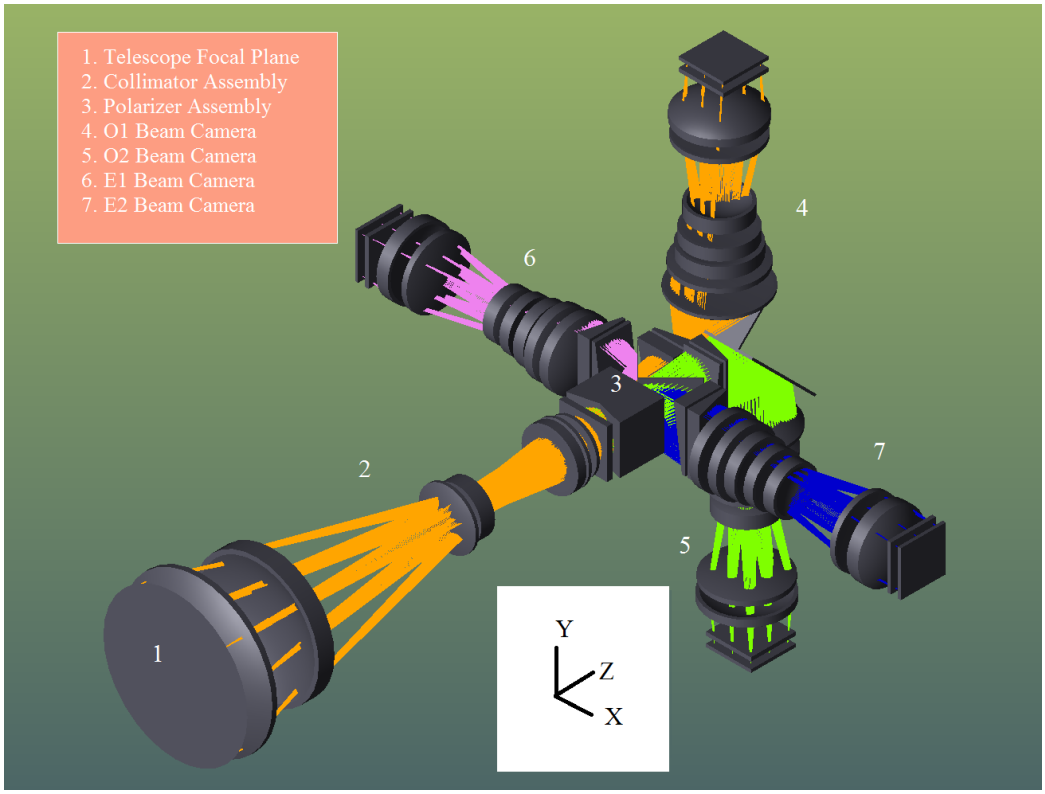

Figure 1. Optical design of the WALOP-South instrument from *Maharana et.al (2021)*[2]

The WALOP-South[2,3] is currently under assembly at IUCAA, India, and is scheduled to be commissioned in the year 2022. At the Sutherland Observatory, where the WALOP-South instrument will be installed, the nighttime temperatures can vary between 10 to - 5°C. Most glasses have a coefficient of thermal expansion (CTE) of around $7 \times 10^{-6}/K$, while the most commonly used metals for making lens mounts, Aluminum and Titanium, have CTEs of $24 \times 10^{-6}/K$ and $8.4 \times 10^{-6}/K$, respectively. So during the operation of the instruments at night, there is relative expansion/contraction between the lens and the lens mount, leading to induced stresses on the glass from the metal mount. Stress can also be induced due to non-zenithal pointing of the lens and lens mount, i.e., when the lens's optical axis is not along the gravity direction.

In addition to thermal gradients and gravity, stresses may also be induced during the fabrication and mounting of the optical components.[4] Stress on glass leads to an anisotropic change in the refractive index of the glass, making it act as a birefringent material.[5–8] The birefringence introduces wavefront error and polarization changes in the light propagating through the system.[9] *Doyle et.al (2002)* have modeled the stress-induced birefringence for a lens and a beam splitter using the optical design software *Code-V* and optomechanical design and analysis software *Sigfit* and estimated the crosstalk variation over the temperature. Modeling of mechanical stress-birefringence for optical plates used in the optical lithography system has been done by *Liu (2020)*[10] using finite element models and ray tracing analysis.

A critical requirement for the WALOP-South instrument is the rigidity of the instrument: it should maintain its optical and polarimetric performance under all conditions of temperature and telescope pointing positions. The effect of the retardance (introduced as a consequence of stress birefringence) on the instrumental polarization can be analyzed through the 4×4 Mueller matrix M_δ[11] given in Eqn 1. The crosstalk between the Stokes parameters is given by $\sin(\delta)$, where δ is the phase retardation. As we aim to attain accuracy of 0.1 %, and almost all stars are polarized to less than 1 % in p in the regions covered by PASIPHAE survey, the maximum allowable δ becomes $\sin(\delta) = \delta = \frac{0.1\%}{1\%} = \frac{1}{10}$. Hence, modeling and estimating stress-induced birefringence is extremely important for a high accuracy polarimetric instrument such as WALOP-South.[8]

$$M_\delta = \begin{bmatrix} 1 & 0 & 0 & 0 \\ 0 & 1 & 0 & 0 \\ 0 & 0 & cos\delta & sin\delta \\ 0 & 0 & -sin\delta & cos\delta \end{bmatrix} \tag{1}$$

This work presents the stress-induced birefringence estimation due to thermal and gravity stresses (following the mathematical model outlined by Doyle et al.[9]) on two lenses in the WALOP-South instrument. First, we calculate the phase and path difference introduced due to birefringence. Then, Mueller matrices are estimated by incorporating the phase to understand the polarization changes through the instrument. Section 2 briefly describes the optical layout and details of the Finite Element Analysis (FEA) simulations carried out in *Solidworks*. Methodology to estimate the Stress birefringence is given in Section 3. Section 4 provides the details of Mueller matrix estimation in *Zemax*. Finally, conclusions and discussions are given in the last section.

2. OPTO-MECHANICAL MODEL OF WALOP-SOUTH AND FINITE ELEMENT ANALYSIS SIMULATIONS

Usually, a finite element mechanical modeling software is used to obtain the stress tensor, and the stress-birefringence and polarization calculations are estimated using an optical design software. Our analysis uses *Solidworks* to estimate the stresses at different node points. The stress data for all the node points are imported and then further processed to estimate the stress birefringence by a dedicated pipeline developed in *Mathematica* programming software. The final polarization calculations are modeled using the optical design software *Zemax*.

Using the optomechanical model of the WALOP-South instrument (as shown in Figure 2), we carried out Finite Element Analysis (FEA) simulations in *Solidworks* to estimate the stresses for two lenses in the collimator (Cl1 and Cl6). The details of the simulations are provided in Table 1. Telescope pointing airmass corresponds to the pointing of zenith and 30° from the horizon.

There are two kinds of lens mounts in WALOP-South: one for large lenses with an aperture greater than 150 mm, and the second for smaller lenses (< 150mm). We consider one of each kind, the first collimator lens (Cl1) that holds the largest lens (250 mm aperture) and the last collimator lens (Cl6) (90 mm aperture) in our analysis. Figure 3 shows the cross-section of the collimator assembly with Cl1 and Cl6 marked. Due to large air separations between successive lenses in the collimator, cylindrical barrels/spacers are used to connect the lens holders.

The lenses are held in their holders using flexure-based lens mounts, which are widely used to achieve and maintain high accuracy alignments.[12] Figure 4 and 5 shows two of the lens holder mounts of the instrument. The design of these mounts was obtained from Finite Element Analysis (FEA) based simulations in the *SolidWorks* software. The lens is attached to the holder using the flexure arms, whose tips are bonded with the rim of the lens

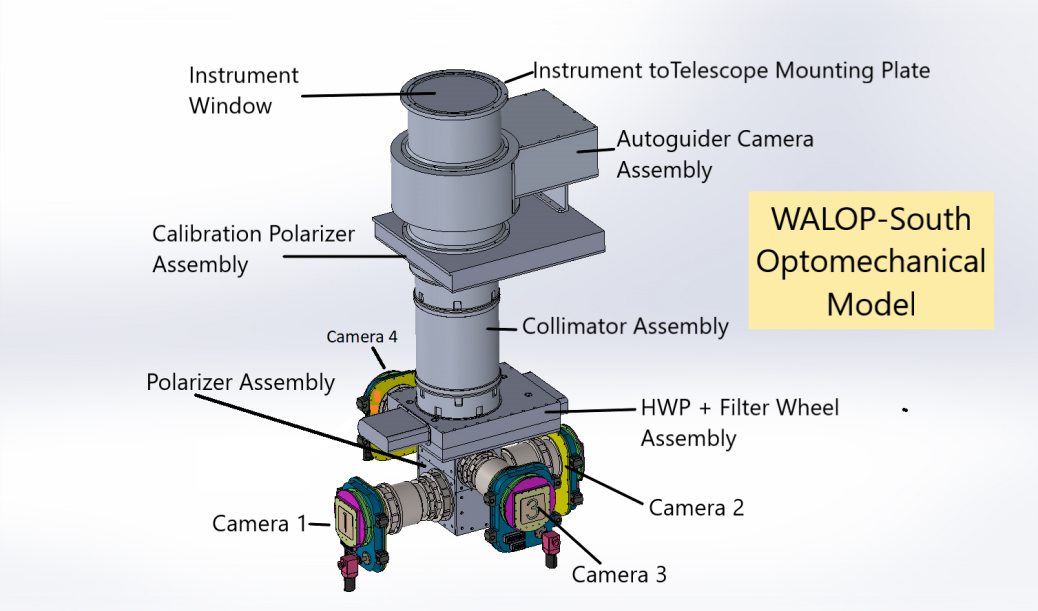

Figure 2. The optomechanical model of the WALOP-South instrument with various subsystems marked. The trusses are provided to control the instrument flexure

Serial Number	Lens Mount Material	Temperature in Celcius	Telescope Pointing Airmass
1	Aluminium 6061-T6	25	1
2			2
3		-5	1
4			2
5	Titanium 6Al-4V	25	1
6			2
7		-5	1
8			2

Table 1. List of simulations done for each lens.

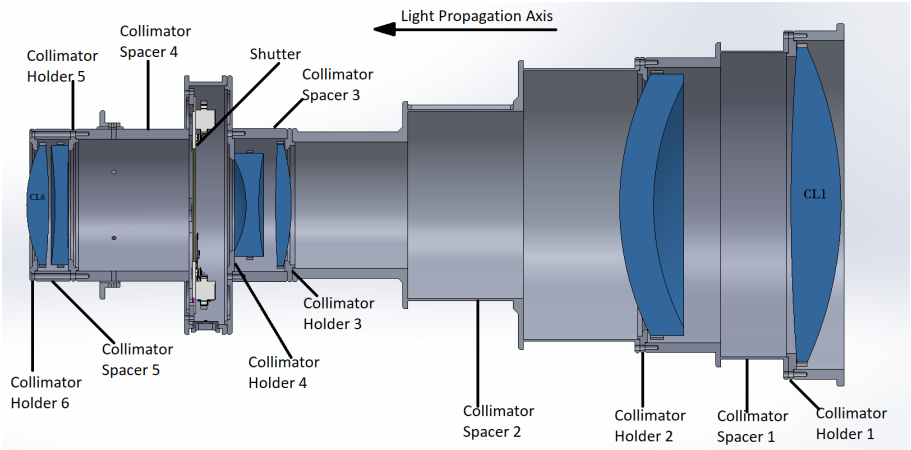

Figure 3. Cross-section of the collimator assembly barrel. Lenses are held in their holder and connected to each other using spacer element. Cl1 (Collimator Lens 1) and Cl6 (Collimator Lens 6) holders are marked.

at multiple points. This constrains all the degrees of freedom of the lens, except radial expansion and contraction in the mounting plane, thus maintaining the alignment irrespective of relative contraction/expansion between the lens and lens holder due to temperature changes. Additionally, these mounts are designed to maintain the centering of the lens to within 4-5 microns with respect to its holder at all orientations, especially when the lens mount is pointing towards the horizon (the worst-case scenario), as will be the nominal orientation of the camera lenses when the instrument is pointing at zenith (please refer to Figure 2).

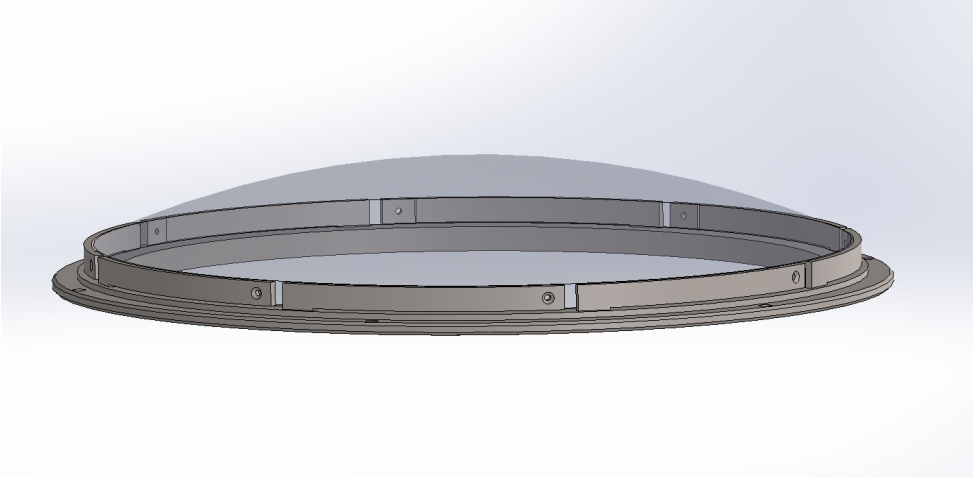

Figure 4. The lens mount used for large aperture lenses ($\phi > 200$ mm): collimator lenses 1 and 2. There are eight flexure arms around the lens' cylindrical rim.

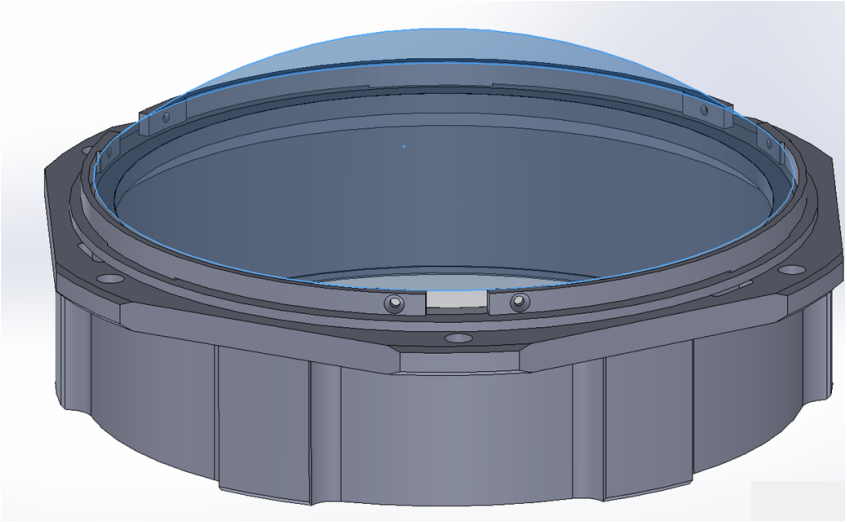

Figure 5. Design of lens mount for smaller aperture lenses ($\phi < 200$ mm), used for all lenses except collimator lenses 1 and 2. It consists of 6 flexure arms around the lens' cylindrical rim.

3. ESTIMATION OF STRESS BIREFRINGENCE

From the FEA simulations in *Solidworks*, we estimate all the six stress components at every node point: three components of normal stresses (σ_x,σ_y,σ_z) and three components of shear stresses (τ_{xy},τ_{xz},τ_{yz}). These six

components form the stress tensor as shown:

$$Stress\ Tensor = \begin{pmatrix} \sigma_x & \tau_{xy} & \tau_{xz} \\ \tau_{xy} & \sigma_y & \tau_{yz} \\ \tau_{xz} & \tau_{yz} & \sigma_z \end{pmatrix} \tag{2}$$

3.1 Principal stresses and principal directions

For certain planes through a material, traction vectors act normal to the plane, and the traction ($\mathbf{T}$) can be expressed as a scalar multiple of the normal vector $\mathbf{n}$ as, $\mathbf{T} = \sigma\mathbf{n}$. These are called the principal planes. Using Cauchy's law, for these planes we have, $\sigma_{ij}\mathbf{n_j} = \sigma\mathbf{n_i}$. This is a standard eigenvalue problem, where σ are the eigenvalues or principal stresses (σ_1,σ_2,σ_3) and $\mathbf{n_i}$ are the eigenvectors which are principal directions. The formalism to obtain principal stresses and their directions are outlined below (which is reproduced from Analysis of three dimensional stress):

$$\begin{pmatrix} \sigma_x & \tau_{xy} & \tau_{xz} \\ \tau_{xy} & \sigma_y & \tau_{yz} \\ \tau_{xz} & \tau_{yz} & \sigma_z \end{pmatrix} \begin{pmatrix} \mathbf{n1} \\ \mathbf{n2} \\ \mathbf{n3} \end{pmatrix} = \sigma \begin{pmatrix} \mathbf{n1} \\ \mathbf{n2} \\ \mathbf{n3} \end{pmatrix} \tag{3}$$

$$\begin{pmatrix} \sigma_x & \tau_{xy} & \tau_{xz} \\ \tau_{xy} & \sigma_y & \tau_{yz} \\ \tau_{xz} & \tau_{yz} & \sigma_z \end{pmatrix} - \sigma \begin{pmatrix} 1 & 0 & 0 \\ 0 & 1 & 0 \\ 0 & 0 & 1 \end{pmatrix} \begin{pmatrix} \mathbf{n1} \\ \mathbf{n2} \\ \mathbf{n3} \end{pmatrix} = \begin{pmatrix} 0 \\ 0 \\ 0 \end{pmatrix} \tag{4}$$

$$\begin{pmatrix} \sigma_x - \sigma & \tau_{xy} & \tau_{xz} \\ \tau_{xy} & \sigma_y - \sigma & \tau_{yz} \\ \tau_{xz} & \tau_{yz} & \sigma_z - \sigma \end{pmatrix} \begin{pmatrix} \mathbf{n1} \\ \mathbf{n2} \\ \mathbf{n3} \end{pmatrix} = \begin{pmatrix} 0 \\ 0 \\ 0 \end{pmatrix} \tag{5}$$

The above system has the solution only if the determinant of the coefficient matrix is zero, that is,

$$det \begin{bmatrix} \sigma_x - \sigma & \tau_{xy} & \tau_{xz} \\ \tau_{xy} & \sigma_y - \sigma & \tau_{yz} \\ \tau_{xz} & \tau_{yz} & \sigma_z - \sigma \end{bmatrix} = 0 \tag{6}$$

We obtain the characteristic equation of the stress tensor using the above equation, solving which we obtain the principle stresses σ_1, σ_2 and σ_3 and principle directions.

We construct the stress tensor for every node in the FEA analysis and obtain the principal stresses for both (Cl1 and Cl6) the lenses for all the scenarios mentioned in Table 1. The results are shown here for one of the extreme cases of temperature and telescope position. Figures 6 and 7 show the principal stresses estimated for the first collimator lens (Cl1) of WALOP-South using Aluminum and Titanium mounts when the telescope is pointing at 30° to the horizon and the operating temperature of -5°C. The stresses are shown for the lens at different diameters (250 mm, 240 mm, and 230 mm) to understand the stress distribution over the clear aperture. The maximum stress value is obtained at the mounting points between the lens and the mount, reducing as we move inwards. The stresses for the Aluminum mount are found to be much higher (an order of 10) compared to the Titanium mount due to the coefficient of thermal expansion.

The principal stresses are shown in Figures 8 and 9 for the last collimator lens (Cl6) using Aluminum and Titanium mounts, respectively. The stresses are shown at three different lens diameters, 94 mm, 82 mm, and 76 mm, to understand the variation of the stresses with lens aperture. The stresses in Cl6 show similar behavior as Cl1 and are found to be lower for the Titanium mount.

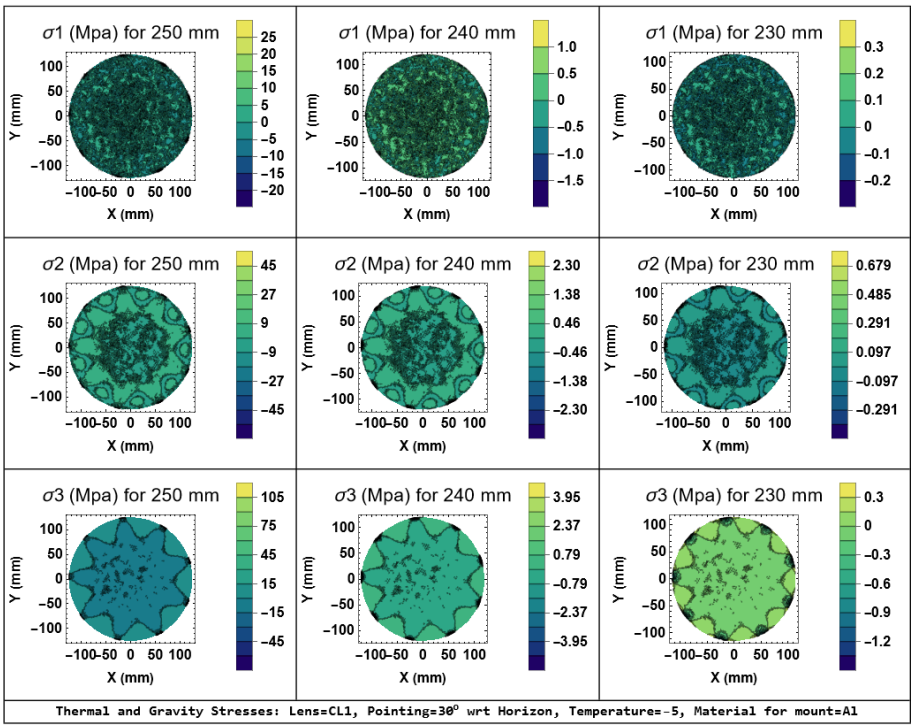

Figure 6. Heat map of the principal stresses shown for the first collimator lens of WALOP-South at different aperture radii using Aluminum as the Lens mount

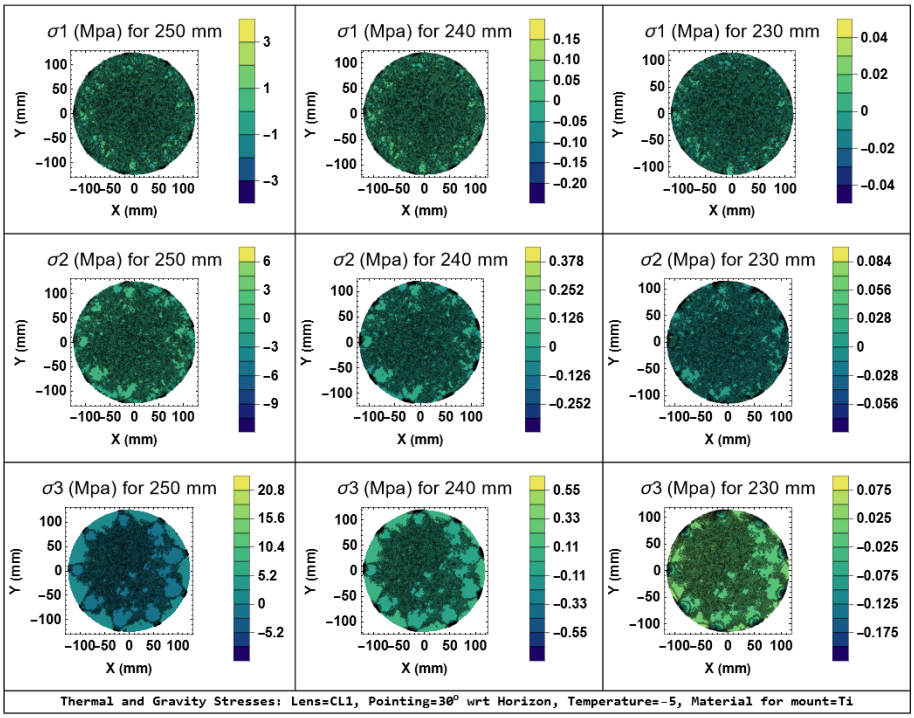

Figure 7. Heat map of the principal stresses shown for the first collimator lens of WALOP-South at different aperture radii using Titanium as the Lens mount

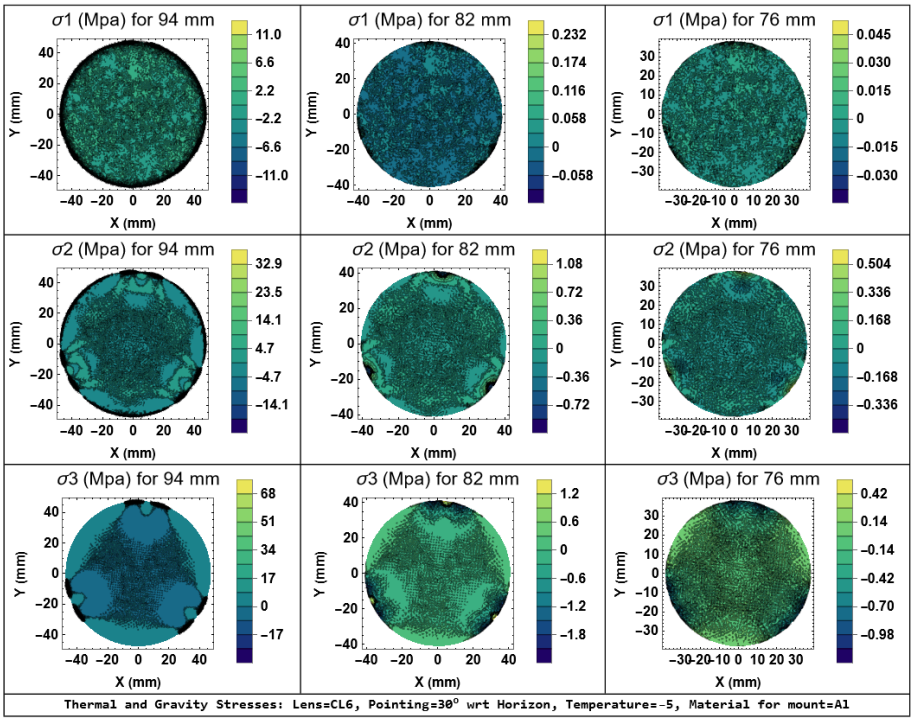

Figure 8. Heat map of the principal stresses shown for the last collimator lens of WALOP-South at different aperture radii using Aluminum as the Lens mount

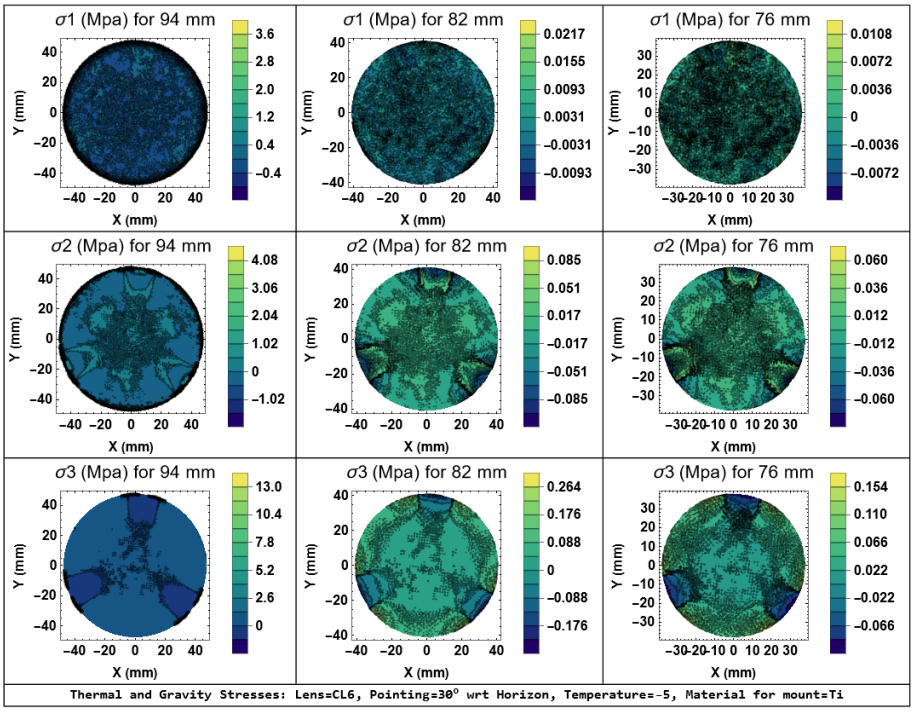

Figure 9. Heat map of the principal stresses shown for the last collimator lens of WALOP-South at different aperture radii using Titanium as the Lens mount

3.2 Stress birefringence

The birefringence can be estimated using the principal stresses σ_1, σ_2 and σ_3 as follows:

$$\Delta n12 = n2 - n1 = k(\sigma_2 - \sigma_1) \tag{7}$$
$$\Delta n23 = n3 - n2 = k(\sigma_3 - \sigma_2) \tag{8}$$
$$\Delta n31 = n1 - n3 = k(\sigma_1 - \sigma_3) \tag{9}$$

where k is the relative stress optics co-efficient, the stress-optical coefficient k is defined as the ratio of birefringence to true stress with units mm^2/N.[13] k is a function of wavelength, glass type, and temperature measured at the ambient temperature of 21°C. For CL1 made of H-BAK8, k=2.62 mm^2/N and CL6 made of S-BAL14, k=2.9mm^2/N. In our simulations, the optical axis of the WALOP-South system is along the z axis. We find that one of the three eigenvectors is along z, while the other two are in a plane parallel to the $x-y$ plane. Only the principal stresses (σ_2 and σ_3) perpendicular to the optical axis are required to estimate the stress birefringence $\Delta n23$.

Figures 10 and 11 show the birefringence estimated for the first and last collimator lens of WALOP-South for the telescope pointing at 30° from the horizon and operating temperature of -5°C for Aluminum and Titanium mounts respectively. As seen from the values of the principal stresses for both the metal mounts, the birefringence for the titanium mount is $\sim$ ten times less than the Aluminum mount. The maximum values of the birefringence are obtained at the bonding point and found to decrease towards the center. These birefringence values are used to estimate the change path difference and thus phase of the light propagating through the lens.

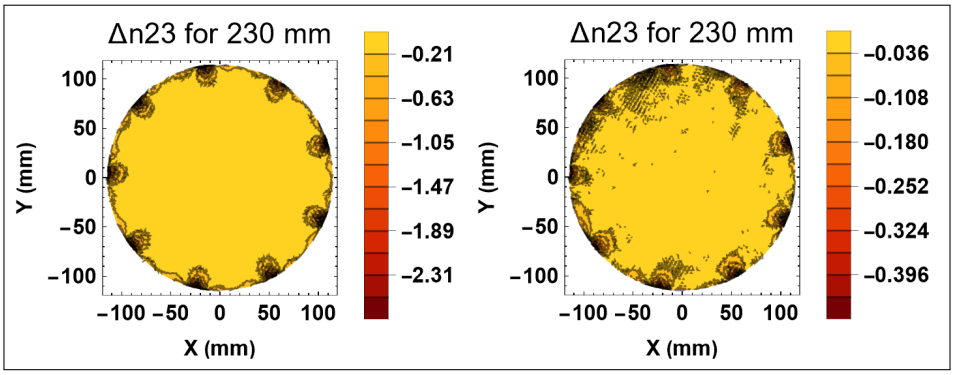

Figure 10. Stress induced birefringence estimated for Collimator Lens 1: Mount:Al (left), Mount: Ti (right)

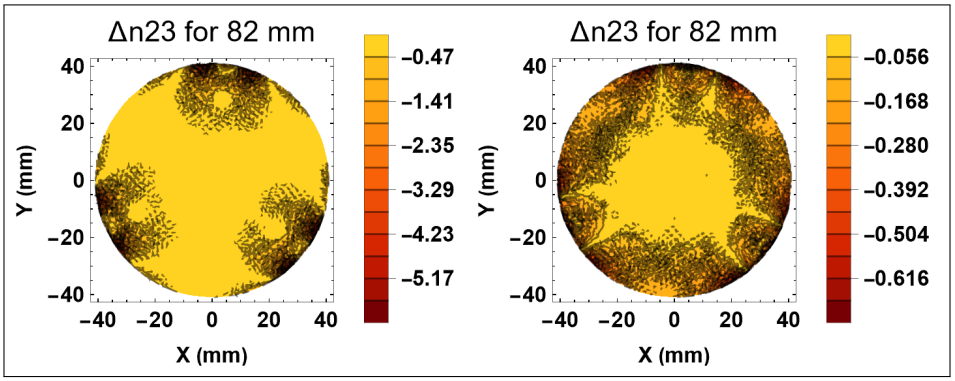

Figure 11. Stress induced birefringence estimated for Collimator lens 6: Mount:Al (left), Mount: Ti (right)

3.3 Estimation of path difference and phase retardation

When light propagates through a birefringent material (birefringence of $\Delta n23$) of thickness t, the path difference (PD) and corresponding phase retardation (δ) can be estimated as:

$$PD = (\Delta n23)t; \quad \delta = \frac{2\pi}{\lambda}(\Delta n23)t \tag{10}$$

We have estimated the path difference and phase retardation for the first and last collimator lens as shown in Figures 12 and 13 respectively. The maximum value of PD is found to be -0.0264λ for cl1 and -0.0176λ for cl6 at λ=600 nm. Except at the mounting points, phase retardation are less than 0.01 radians throughout clear aperture of the lens.

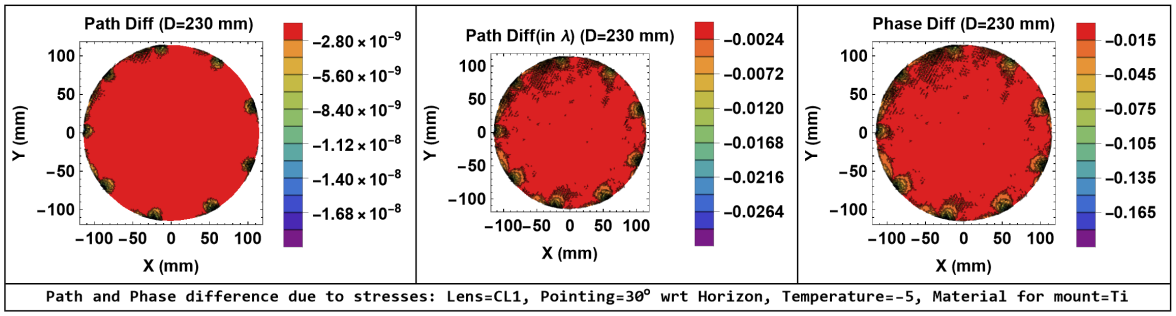

Figure 12. Path and phase difference estimated for Collimator lens 1

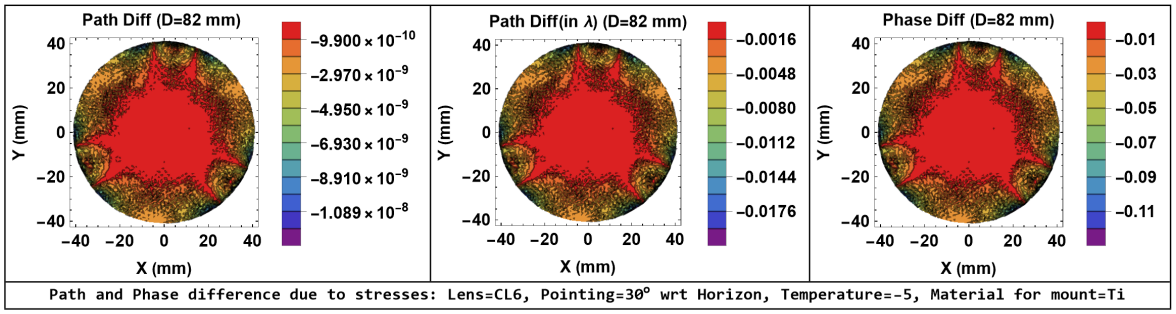

Figure 13. Path and phase difference estimated for Collimator lens 6

The summary of the results for all the scenarios listed in Table 1 is provided in Table 2 for the first collimator lens and Table 3 for the last collimator lens. We provide the maximum values estimated for each of the parameters. It can be seen that for T=25°C, the values obtained for Aluminum and Titanium mounts are very similar. Even when gravity stresses are considered at T=25°C, the values of the principal stresses, birefringence, path, and phase difference are in the same order. Comparing the values for T=-5°, we find that the values for the Aluminum mounts are higher (an order of $\sim$ 10) compared to the Titanium mounts. Hence, thermal stresses are the main reason for the stress birefringence in the WALOP-South lenses.

4. SIMULATIONS IN ZEMAX: ESTIMATION OF MUELLER MATRIX

The phase retardation (δ) is used to obtain the Mueller matrix, M_δ. We also perform polarization ray tracing in *Zemax* to estimate the Mueller matrix without the stress birefringence, M_{act}. The Mueller matrix, including the effect of birefringence (M_{st}), is given by:

$$M_{st} = M_\delta \cdot M_{act} \tag{11}$$

T	Mount	Pointing	P1	P2	P3	n12	n23	n31	Path diff	Phase diff
(°C)			(Mpa)	(Mpa)	(Mpa)				(in λ)	(radians)
25	Al	Zenith	0.0155	0.06	0.085	-0.18	-0.144	0.264	-0.00924	-0.0572
25	Ti	Zenith	0.0216	0.06	0.102	-0.165	-0.144	0.264	-0.00924	-0.0583
25	Al	30°wrt horizon	0.01	0.0305	0.06	-0.088	-0.099	0.18	-0.0066	-0.0407
25	Ti	30°wrt horizon	0.01	0.031	0.07	-0.0891	-0.0968	0.192	-0.00638	-0.0407
-5	Al	Zenith	0.497	0.88	-1.28	-1.2	-2.42	3.24	-0.168	-1.023
-5	Ti	Zenith	0.0504	-0.186	0.396	-0.495	-0.836	1.08	-0.055	-0.341
-5	Al	30°wrt horizon	0.294	0.679	-1.2	-1.32	-2.31	3.24	-0.154	-0.968
-5	Ti	30°wrt horizon	0.034	0.084	-0.175	-0.192	-0.396	0.504	-0.0264	-0.165

Table 2. Summary of the values obtained for the lens Cl1 for different scenarios listed in Table 1

T	Mount	Pointing	P1	P2	P3	n12	n23	n31	Path diff	Phase diff
°C			(Mpa)	(Mpa)	(Mpa)					(radians)
25	Al	Zenith	0.00275	0.015	-0.0252	-0.0451	-0.0363	0.0864	-0.00108	-0.00671
25	Ti	Zenith	0.00265	0.015	-0.0252	-0.0462	-0.0363	0.0864	-0.00108	-0.00671
25	Al	30°wrt horizon	0.00258	0.0085	0.0217	-0.0286	-0.0451	0.0732	-0.00132	-0.00836
25	Ti	30°wrt horizon	0.00264	0.0085	0.0093	-0.0286	-0.044	0.072	-0.00132	-0.00803
-5	Al	Zenith	0.232	1.14	1.2	-3.19	-5.17	6	-0.154	-0.968
-5	Ti	Zenith	0.024	0.08	0.258	-0.253	-0.605	0.792	-0.0176	-0.11
-5	Al	30°wrt horizon	0.232	1.08	-1.8	-3.08	-5.17	6	-0.156	-0.957
-5	Ti	30°wrt horizon	0.0217	0.085	0.264	-0.275	-0.616	0.852	-0.017	-0.11638

Table 3. Summary of the values obtained for the lens Cl6 for different scenarios listed in Table 1

We look at the difference of the Mueller matrix elements (M_{act}-M_{st}) to understand the change caused in the polarization values due to the stress-induced birefringence. Figures 14 and 15 show the difference of the Mueller matrix elements for the first collimator lens when the instrument is pointing at 30° with respect to horizon and $T = -5C$. We have shown 3×3 Mueller matrix elements as WALOPs are designed to measure linear polarization. The first two rows of the Mueller matrix show no effect due to the stress birefringence, which implies that the measurement of Stokes q is not affected by the birefringence introduced. Looking at the third row of the Mueller matrix, we find low order residuals only at the edge of the field for $M31$ and $M32$ for both Aluminum and Titanium mounts. The term $M33$ shows a residual of about 18% and 5% for Al and Ti, respectively.

5. SUMMARY AND CONCLUSIONS

We have estimated the stress birefringence for two lenses in the collimator of the WALOP-South instrument. We have analyzed the scenarios of thermal and gravity stresses for Aluminum and Titanium mounts. Through the analysis, we find that the telescope pointing leading to gravity stresses does not make much difference in the stresses in the lenses. In contrast, temperature changes introducing thermal stresses are the main reason for the stress birefringence. We have also estimated the path and phase difference due to the birefringence and their effect on the polarization measurements.

As expected, we find higher stresses in the lens mounts made of Aluminum. Nevertheless, the retardance is 0.1 or less throughout the clear aperture for both the mounts. The residuals of the Mueller matrix elements are zero throughout the clear aperture for most of the terms except $M33$. As larger lenses are difficult and costlier to fabricate, we decided to make their mounts with Titanium to minimize the thermal stress on the lenses.

Similar to the first collimator lens, stresses are higher in the lenses with Aluminum mounts (within the allowable strength limit of glass), and the retardance is less than 0.1 throughout the clear aperture (82 mm) for both the mounts in the case of the last collimator lens. As most lenses will use these kinds of mounts, to reduce the instrument's weight and achieve better machining accuracy, we decided to use Aluminum for smaller lenses.

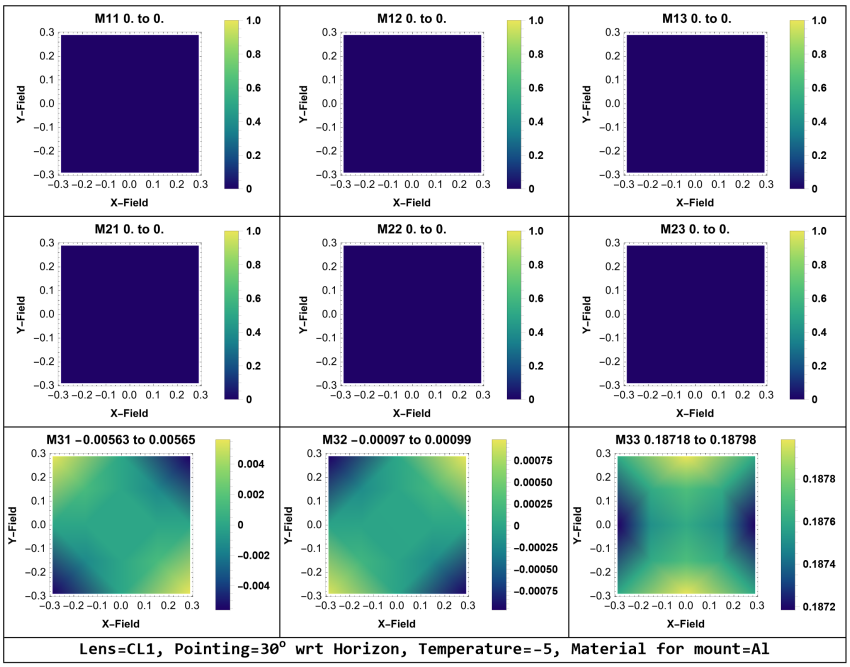

Figure 14. Difference of the Mueller matrix elements (M_{act}-M_{st}) for Aluminum mount for Cl1 over the 30× 30 field of view (fov) of WALOP-South. The zero obtained for the top two rows of the Mueller matrix shows that δ has no effect on the measurement of Stokes parameter, q. We find residual to be zero for the maximum part of the fov for $M31$ and $M32$.

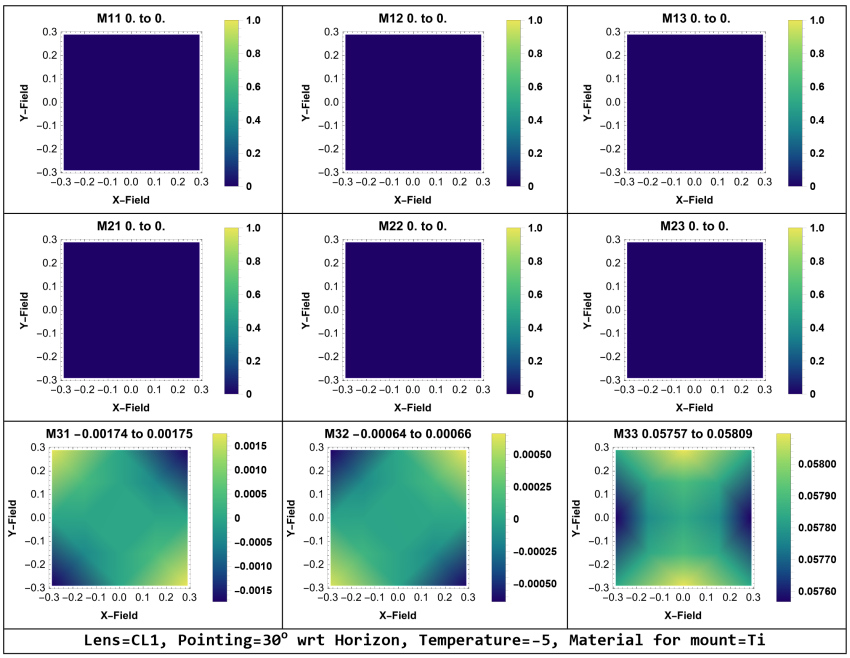

Figure 15. Difference of the Mueller matrix elements (M_{act}-M_{st}) for Titanium mount for Cl1 over the 30× 30 field of view of WALOP-South. The zero obtained for the top two rows of the Mueller matrix shows that δ has no effect on the measurement of Stokes parameter, q. We find residual to be zero for the maximum part of the fov for $M31$ and $M32$.

ACKNOWLEDGMENTS

The PASIPHAE program is supported by grants from the European Research Council (ERC) under grant agreement No 771282 and No 772253, from the National Science Foundation, under grant number AST-1611547

and the National Research Foundation of South Africa under the National Equipment Programme. This project is also funded by an infrastructure development grant from the Stavros Niarchos Foundation and from the Infosys Foundation.

REFERENCES

[1] Tassis, K., Ramaprakash, A. N., Readhead, A., Potter, S. B., Wehus, I. K., Panopoulou, G. V., Blinov, D., Eriksen, H. K., Hensley, B., Karakci, A., et al., "Pasiphae: A high-galactic-latitude, high-accuracy optopolarimetric survey," *arXiv preprint arXiv:1810.05652* (2018).

[2] Maharana, S., Kypriotakis, J. A., Ramaprakash, A. N., Rajarshi, C., Anche, R. M., Shrish, S., Blinov, D., Eriksen, H. K., Ghosh, T., Gjerløw, E., et al., "Walop-south: a four-camera one-shot imaging polarimeter for pasiphae survey. paper i—optical design," *Journal of Astronomical Telescopes, Instruments, and Systems* **7**(1), 014004 (2021).

[3] Maharana, S., Kypriotakis, J. A., Ramaprakash, A. N., Khodade, P., Rajarshi, C., Joshi, B. S., Chordia, P., Anche, R. M., Mishra, S., Blinov, D., Eriksen, H. K., Ghosh, T., Gjerløw, E., Mandarakas, N., Panopoulou, G. V., Pavlidou, V., Pearson, T. J., Pelgrims, V., Potter, S. B., Readhead, A. C. S., Skalidis, R., Tassis, K., and Wehus, I. K., "WALOP-South: A wide-field one-shot linear optical polarimeter for PASIPHAE survey," in [*Ground-based and Airborne Instrumentation for Astronomy VIII*], Evans, C. J., Bryant, J. J., and Motohara, K., eds., **11447**, 1135 – 1146, International Society for Optics and Photonics, SPIE (2020).

[4] Spilman, A. K. K., [*Stress-engineered optical elements*], University of Rochester (2008).

[5] Yi, A., Tao, B., Klocke, F., Dambon, O., and Wang, F., "Residual stresses in glass after molding and its influence on optical properties," *Procedia Engineering* **19**, 402–406 (2011).

[6] Kuske, A. and Robertson, G., "Photoelastic stress analysis(book)," *Research sponsored by the Deutsche Forschungsgemeinschaft. London and New York, John Wiley and Sons, 1974. 531 p* (1974).

[7] Bach, H. and Neuroth, N., [*The properties of optical glass*], Springer Science & Business Media (1998).

[8] Wang, W.-C., "Photoelasticity," *Department of Mechanical Engineering. University of Washington* (1990).

[9] Doyle, K. B., Hoffman, J. M., Genberg, V. L., and Michels, G. J., "Stress birefringence modeling for lens design and photonics," in [*International Optical Design Conference*], IWC1, Optical Society of America (2002).

[10] Liu, T., Hu, J., Zhu, L., Zhou, R., Zhang, C., Gu, L., Sun, X., Yu, J., Zeng, A., and Huang, H., "Mechanical stress birefringence of optical plates," *Applied Optics* **59**(24), 7371–7375 (2020).

[11] Goldstein, D. H., [*Polarized light*], CRC press (2017).

[12] Vukobratovich, D. and Richard, R. M., "Flexure mounts for high-resolution optical elements," in [*Optomechanical and Electro-Optical Design of Industrial Systems*], **959**, 18–36, SPIE (1988).

[13] Galiatsatos, V., [*Refractive Index, Stress-Optical Coefficient, and Optical Configuration Parameter of Polymers: Datasheet from · Volume : "Physical Properties of Polymers Handbook" in SpringerMaterials (https://doi.org/10.1007/978-0-387-69002-5_50)*], Springer Science+Business Media, LLC. Copyright 2007 Springer Science+Business Media, LLC.